

The spatial statistics of turbulent dissipation rates

James Glimm and Vinay Mahadeo
*Department of Applied Mathematics and Statistics,
 Stony Brook University,
 Stony Brook, NY 11794
 (Dated: March 11, 2022)*

We study the spatial statistics of velocity gradient volatility (i.e., the energy dissipation rate) in turbulent flow. We extend the Kolmogorov-Obukhov theory but also narrow its scope. The models are log normal, with verification from finely resolved large eddy and direct numerical simulations. They are parameterized by a mean and a covariance operator. Addressing applications to large eddy simulations, the mean and the covariance depend on the resolved scale solution. Removing this resolved scale dependence by a locally defined rescaling of the turbulent statistics yields a universal theory for the subgrid statistics, specifically for the mean and variance of turbulent fluctuations, i.e., the log of the energy dissipation rate ϵ . The variance of the velocity gradient statistics is found to be log normal, in accordance with Kolmogorov 1962. Rescaling by the resolved scale mean and variance removes the influence of the resolved scales on the subgrid scales, justifying conceptually the universality we observe. The universality is the basis of new power scaling laws. The new power laws, in turn, allow a simple parameterization of the mean and covariance of the subgrid rescaled dissipation rate, i.e., velocity gradient volatility. We treat the coarse grid resolved space-time location as a random variable. A restriction of the theory to a small range of unresolved but stochastically modelled scales is proposed, with renormalization group ideas offered to overcome this restriction.

INTRODUCTION

The scaling law of Kolmogorov [4], although simple, is among the deepest contributions to the understanding of turbulent flow. Turbulent flow is generally considered to be the major outstanding problem of classical physics. We propose new parameterized spatial statistics and scaling laws for turbulent fluctuations which extend ideas of the Kolmogorov 1962 (K62) theory but also narrow its scope. Verification is from comparison to Direct Numerical Simulation (DNS). Because we do not assume homogeneity or isotropy of the flow, the theory is applicable to the unresolved scales of Large Eddy Simulations (LES), and is a stochastic subgrid scale (SGS) model. A major contribution of the theory presented here is to capture SGS fluctuations, in addition to the means computed from traditional SGS theories.

We assume single fluid, constant density, incompressible flow, governed by the Navier-Stokes equation. The scalar dissipation rate is defined as

$$\epsilon = \frac{\nu}{2} \sum_{i,j} \left(\frac{\partial \mathbf{u}_i}{\partial \mathbf{x}_j} + \frac{\partial \mathbf{u}_j}{\partial \mathbf{x}_i} \right)^2 = \frac{\nu}{2} \|S + S^*\|_2^2, \quad (1)$$

with ν the dynamic viscosity, \mathbf{u} the fluid velocity, and

$$S = \frac{\partial \mathbf{u}_i}{\partial \mathbf{x}_j} \quad (2)$$

the strain rate.

Properties of ϵ are fundamental to a number of deep theories of turbulence, including notions of turbulent intensity, turbulent intermittency [10], corrections to the Kolmogorov 5/3 exponent and scaling laws for velocity

moments. The analysis of ϵ has been applied to turbulent diffusion, short distance asymptotics for the velocity two point correlation function, and prediction of a fractal or multifractal spatial distribution of regions of high turbulent intensity, with the turbulent regions concentrated in a fractal set of dimension $D < 3$ [2]. Scaling laws for wall bounded turbulence (a topic not addressed here) are discussed in [1]. There is an extensive literature on the above topics, which we do not attempt to document in this article. See the survey article [3] for elaborations and further references. Kolmogorov [5] and Obukhov [7] conjectured that ϵ obeys a lognormal distribution at sufficiently high Reynolds numbers.

Our main results are new scaling law for the mean and covariance of $\chi = \ln(\epsilon)$, which we designate as turbulent intensity. The scaling laws originate in a universality principle, of the mean μ and the variance of χ for inertial degrees of freedom. The connection between universality, which would seem to require isotropic homogeneous turbulence, and subgrid scales of LES, which can be very far from homogeneous or isotropic is one of our central results. Depending on the local properties of the resolved scales of turbulence, we introduce a rescaling of the turbulent statistics, and it is only after this rescaling that the subgrid scales of turbulence become universal. In fact, universality does have limits, in terms of the number of subgrid scales it can accommodate. In our numerical tests, we consider 3 levels of mesh refinement, that is a change of length scales by a factor of 8. For a large number of length scales, we have in mind a renormalization group methodology, with successive integration over smaller length scales, and a resetting of parameters using the (statistical) knowledge of the already integrated

scales, a point of view to be elaborated in future work.

In Sec. , we specify the simulation study used for verification of the theories proposed here. We define the statistics and the ensemble used. We show that ϵ has log normal statistics (and χ has normal statistics).

The spatial statistics for ϵ and χ are characterized by the mean μ and covariance Σ^2 of χ . We compare a coarsely gridded LES to a finely gridded LES or DNS. The fine grid extension of the coarse grid solution is of course unique and not stochastic, but we add statistics in the dependence of this extension on the resolved coarse grid cell from which it is derived. The statistics of the fine grid extension for χ depends on the coarsely gridded resolved solution.

A detailed analysis of the χ statistics is carried out in Fourier space, in Sec. . The analysis uses the coarse grid resolved scales as a random variable, to define the statistical properties of the subgrid scales. Our premise is that the spatial aspects of this dependence are largely captured by a resolved scale variance Σ_0^2 and mean μ_0 for χ . When the Σ_0^2 and μ_0 dependency is removed from the refined solution extension by rescaling, the resulting statistics for χ , i.e., Σ^2/Σ_0^2 , is modeled as universal, with Σ^2/Σ_0^2 diagonal and subject to simple modeling assumptions, including new power laws, with only a few $\mathcal{O}(1)$ dimensionless parameters to govern its spatial statistics, all physically understandable. The power laws result from a universality principal for the rescaled statistics. These approximations are confirmed by the fine grid comparison.

Sec. extends this log normal theory to individual components of the strain matrix S and to the tensor dissipation rate. A discussion of results and an outlook for future work is given in Sec. .

THE SPATIAL STATISTICS

The simulation study

All verification tests are based on a series of coarse and finely gridded simulations. The finely gridded LES/DNS study has over two decades of resolution, with the coarsely gridded LES fraction of the solution varying with the simulation parameters. The coarsely gridded LES includes portions of the inertial range and has up to a decade of unresolved inertial range scales to which our modeling applies.

Our fine and coarse grid simulations are conducted with the code [9], using periodic boundary conditions and forced turbulence in a domain size L^3 , $L = 0.05m$, with the viscosity (of air), $1.9e^{-5}m^2/s$. The mesh parameters for three simulations are given in Table I. The resolved levels of turbulence in this numerical study are not extreme.

TABLE I. Mesh parameters for three fine grid and corresponding coarse grid simulations considered in this study.

Fine grid simulation	Fine and coarse grid meshes	Re	Taylor Re	Kolmogorov scale
DNS	256^3 and 32^3	561	40	$1.4 \times \Delta_f$
LES	256^3 and 32^3	1577	67	$0.67 \times \Delta_f$
LES	256^3 and 32^3	2539	85	$0.04 \times \Delta_f$

Let Δ_c denote the coarse grid mesh size, and Δ_f the fine grid mesh size, so that $\Delta_c = 8\Delta_f$. As we are concerned with velocity gradients, which require two mesh cells as a minimum stencil size for their evaluation, we also introduce what we call the resolved coarse and fine grid mesh scales, with $\Delta_r = 2\Delta_c$ as the resolved coarse grid mesh and

$$\Delta_r = 2\Delta_c = 8 \text{ (Resolved } \Delta_f) = 16\Delta_f. \quad (3)$$

Here the resolved fine grid level is $2\Delta_f$, needed to evaluate the fine grid velocity gradients occurring in ϵ and χ .

The statistical ensemble

As with turbulent flow in general, ϵ and χ can be regarded as random fields. In the LES context, ϵ and χ are known (deterministic) at the resolved scales, while their subgrid scale fluctuations can be modeled using spatial statistics. We write the fine grid resolved spatial mesh coordinate $i = i_r, i_s$, where i_r is the coarse grid resolved mesh portion of i . As the resolved coarse mesh spacing is $2\Delta_c$, i_r spans all the coarse grid LES cells other than the last or finest of them. i_s is the remainder, occurring in the fine but not the coarse LES grid resolution and also within the finest level of the LES simulation. There are then $n_r = 16^3$ i_r values and 8^3 i_s values. Note that 2^3 Δ_f mesh indices are missing, as we discuss resolved, not simulation mesh indices.

Our plan is to treat χ , regarded as a fiction of i_s , as random, depending on the random variable i_r . The natural domain for its mean and covariance μ and Σ^2 is the Hilbert space \mathcal{H} of subgrid functions, i.e., functions indexed by i_s but restricted to a single resolved coarse grid cell and having mean zero there. μ is a vector in \mathcal{H} and Σ^2 is an $i_s \times i_s$ positive definite matrix acting on \mathcal{H} .

The statistics are collected as an average over all the possible n_r values of i_r .

The log normal property

We present numerical evidence to support the hypothesis that the fine grid extension of the resolved χ defines a

Gaussian random field, with the mean and covariance defined from averages of distinct resolved coarse grid cells.

The time dependent spatial average of χ has been tested for normality, see [6, 8, 11] and references cited there, based on experimental and DNS evidence. Our verification method to establish the Gaussian property is also based on DNS evidence. A multivariate random variable is Gaussian if its inner product with any fixed vector is univariate Gaussian. Here we consider, as representative choices, the fixed vectors defined by single DNS cell indices i_s .

We use QQ plots to assess univariate normality. In these, the trial distribution is transformed first by a change of the χ independent variables to have zero mean and unit variance. Then we apply an inverse Gaussian change of trial distribution dependent variables, with the result compared to a unit slope straight line.

We create a single QQ plot by holding the fine grid mesh resolved cell indices i_s fixed (16^3 choices), and using the multiple i_r values from the 16^3 resolved coarse grid cells to form the ensemble. In Fig. 1 we superimpose all QQ plots for all choices of i_s as typical tests of normality, demonstrating agreement to a Gaussian law up to $\pm 2\sigma$, a range of agreement consistent with the 4% accuracy expected from the ensemble size.

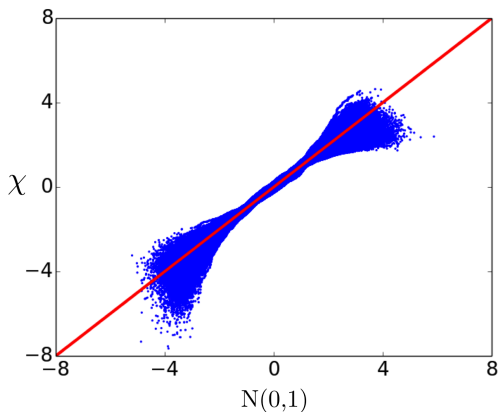


FIG. 1. QQ plot of the fine grid χ distribution in localized resolved cells compared to a normal distribution. Integral scale $Re = 1577$. Both axes are in units of standard deviation. The agreement is good up to ± 2 standard deviations, which is the limit of accuracy imposed by the size of the data sample.

The mean and covariance

The coarse grid resolved level variance of χ is basic to our rescaling strategy. At the level of each coarse grid resolved grid cell, the variance Σ_0^2 of $\chi(i_r)$ is defined as

$$\Sigma_0^2 = (\chi(i_r) - \mu_0)^2 \quad (4)$$

with the definitions $\mu_0 = \overline{\chi(i_r)} = n_r^{-1} \sum_{i_r} \chi(i_r)$.

Consider the fine grid values $\chi(i_r, i_s)$ for the resolved coarse grid $\chi(i_r)$. As a normal random variable, the statistics of χ is characterized by its mean and its covariance. To obtain universal statistics, we rescale χ by subtracting the resolved coarse grid mean and dividing by the standard deviation defining $\hat{\chi}(i_r, i_s) = (\chi(i_r, i_s) - \mu(i_s))/\Sigma_0(i_r)$. The mean μ of χ is

$$\mu(i_s) = n_r^{-1} \sum_{i_r} \chi(i_r, i_s) . \quad (5)$$

The universal, rescaled, statistics are the statistics of $\hat{\chi}$. We follow a similar definition for the covariance, $\hat{\Sigma}^2$ of $\hat{\chi}$,

$$\hat{\Sigma}^2(i_s, j_s) = \overline{\hat{\chi}(i_r, i_s) \hat{\chi}(i_r, j_s)} . \quad (6)$$

where the overbar denotes averaging over all resolved coarse grid cells, namely

$$\overline{(\cdot)} = n_r^{-1} \sum_{i_r} (\cdot) . \quad (7)$$

Furthermore, we will normalize $\hat{\Sigma}^2$ by $\hat{\Sigma}^2(i_r, i_r) = \hat{\Sigma}^2(i_r) = \overline{\hat{\Sigma}_0^2}$, the resolved scale variance, reducing the Reynolds number dependence of $\hat{\Sigma}$.

SPATIAL STATISTICS IN FOURIER SPACE

We propose a Fourier space analysis for μ and $\hat{\Sigma}^2$. As these variables are independent of the resolved variables, they are, in this approximation, periodic within each resolved cell. Thus their Fourier transforms depend on the Fourier modes within a single resolved cell.

In preparing figures in this section, we present functions of \mathbf{k} , unless otherwise noted, after binning all \mathbf{k} values into bins labeled by the scalar wave number k with 200 bins whose size is linear in $\ln k$.

μ in Fourier space

In Fig. 2, we plot $\mu(k)$ vs. k in $\ln \ln$ scaled variables. Observe the approximate scaling law $\mu(k) \sim k^{-d}$, with corrections coming from the dissipation range of scales. Included in the plot is a model curve of the form

$$\mu(k) \sim k^{-d} \quad (8)$$

The coefficients in this model fit are tabulated in Table II.

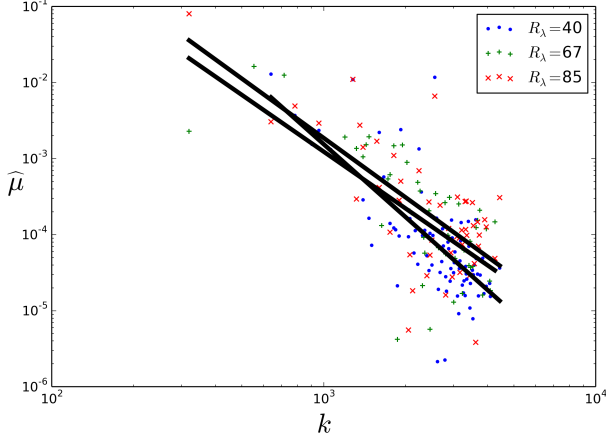


FIG. 2. Plot of $\hat{\mu}(k)$ vs. k (unbinned) for three R values. The few values of $\hat{\mu}$ less than zero are omitted.

TABLE II. Coefficients for the mean model scaling law, for three values of Re .

Re	561	1577	2539
d	3.1	2.5	2.6

Σ^2 in Fourier space

In Fig. 3, we plot the diagonal and off diagonal elements of the covariance matrix $\hat{\Sigma}^2(\mathbf{k}, \mathbf{l})$ for Reynolds number 2549. The smooth curve in the upper part of the figure represent the plot of the diagonal elements as a function of the frequency k , while the noisy data near the bottom of the plot are the collection of all off diagonal elements, plotted vs. $(k+l)/2$. The other Reynolds numbers give similar plots. We conclude that the covariance is, within a good approximation, diagonal.

Our modeling for $\hat{\Sigma}^2$ (and for related operators describing the strain matrix S and its individual matrix entries in Sec.) is based on a simple approximation, which appears to be consistent with the DNS data as examined here. We note that the two random variables contributing to the covariance Σ^2 are orthogonal for $\mathbf{k}_s \neq \mathbf{l}_s$ and so the $\mathbf{k}_s \neq \mathbf{l}_s$ terms vanish. In other words, the Fourier coefficient of $\Sigma^2(i_s, j_s)$ is $\Sigma^2(\mathbf{k}_s, \mathbf{k}_s)$, which we write as $\Sigma^2(\mathbf{k}_s)$. In our DNS case, $\hat{\Sigma}^2$ is a $16^3 \times 16^3$ matrix before binning.

TABLE III. Coefficients for the variance model scaling law, for three values of Re .

Re	561	1577	2539
C_2	5.3	3.9	4.7
C_4	2.6	5.3	7.3

TABLE IV. Representative coefficients of the scaling laws for the dissipation matrices.

	S_{ij}^2					
	$i = j$			$i \neq j$		
Re	561	1577	2539	561	1577	2539
C_2	4.9	3.9	3.7	5.0	4.5	3.1
C_4	1.2	2.0	2.3	1.4	2.3	2.6

	$S^* S$					
C_2	2.6	4.1	4.2	4.6	3.7	4.0
C_4	1.4	2.6	3.2	1.4	2.9	3.6

	SS^*					
C_2	4.8	4.2	3.2	4.4	4.6	3.9
C_4	1.4	2.6	3.6	1.4	2.9	3.6

The Fourier coefficients for $\hat{\chi}$ for distinct angular variables $\mathbf{k}/\|\mathbf{k}\|$ are statistically independent. For distinct values of the scalar Fourier amplitude $k = \|\mathbf{k}\|$, we also assume statistical independence. These assumptions lead to a simple model for $\hat{\Sigma}^2$, tractable for practical use.

We regard the wave number k as an observable on the random field $\hat{\chi}$, with the variance $\hat{\Sigma}^2(k)$ for this observation. We derive k dependent scaling laws. Approximately, the subspace of the Hilbert space in which $\hat{\Sigma}^2(k)$ is defined has dimension proportional to $4\pi k^2$, namely the area of a sphere in momentum space of radius k . Assuming equipartition of the variance of χ within this subspace, the inverse covariance is a multiple of the identity there. We extend the variance equipartition hypothesis, meaning a uniform level of variance, to distinct k values. The subspace variance is then proportional to k^{-2} .

From a more probabilistic point of view, we regard the observation as the result of asking $\mathcal{O}(k^2)$ questions, postulated to be independent: what is the variance of χ associated with each \mathbf{k} lying on the sphere of radius k ? Combining the variance of $\mathcal{O}(k^2)$ independent quantities gives the same answer.

Volume scaling laws apply to the volume dependent coefficients in the scaling law for $\hat{\Sigma}^2$, and use a similar reasoning. Thus, again assuming equipartition, the mesh cell averages over a single coarse grid resolved cell scale with Δ_r^3 . In summary, we propose scaling laws for $\hat{\Sigma}^2(k)dk$ in terms of the scalar wave number k and spatial volume, with the dispersion relation

$$\frac{\hat{\Sigma}^2(k)}{\hat{\Sigma}_0^2} = (\Delta_r^3 4\pi C_2^2 k^2 \exp(C_4^2 \eta^2 k^2))^{-1} \quad (9)$$

with dimensionless constants C_2, C_4 to be determined. The factors Δ_r^3 and $4\pi k^2 dk$ are volumes for physical space and Fourier space. The C_4 term, not previously discussed, is postulated to capture the leading order viscous corrections to the otherwise purely inertial range theory.

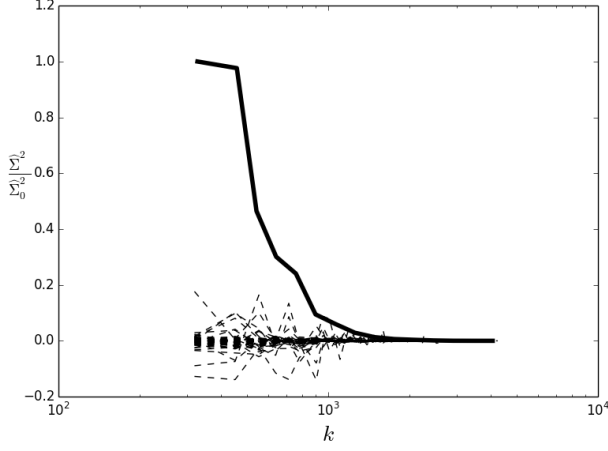


FIG. 3. Plot of diagonal and off diagonal elements of the covariance $\hat{\Sigma}^2(k, l)$ at $Re = 2539$ as a function of frequency $(k + l)/2$. We observe a near vanishing of the off diagonal elements vs. the diagonal elements. The same behavior is observed for the other two Reynolds numbers, but omitted from this plot.

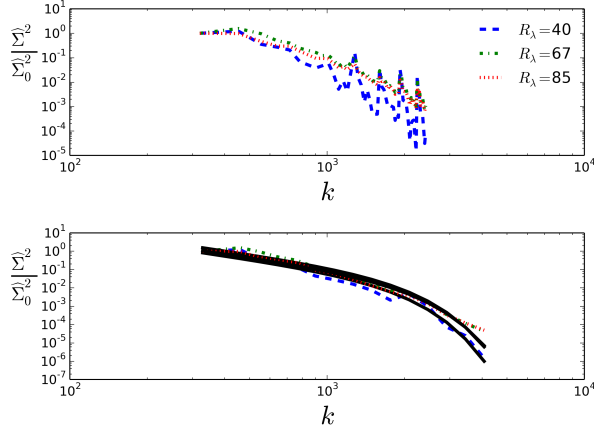


FIG. 4. In-In plot of the diagonal elements of $\hat{\Sigma}^2(k)$ vs. k at different Taylor scaled Reynolds numbers as a function of frequency. Top: unbinned curves. Bottom: binned curves. Solid black lines represent the fitting of the form (9).

In Fig. 4, we plot $\hat{\Sigma}^2(k)$ vs. k on $\ln \ln$ scales with the model curves (9) superimposed, based on optimal choices of the coefficients C_i . We first fit C_2 in the inertial range (small k values), and then fit C_4 over a $1/2$ decade at the end of the inertial range. We observe that most of the Reynolds number dependence of the C_i has been removed by the scaling introduced here, see Table II.

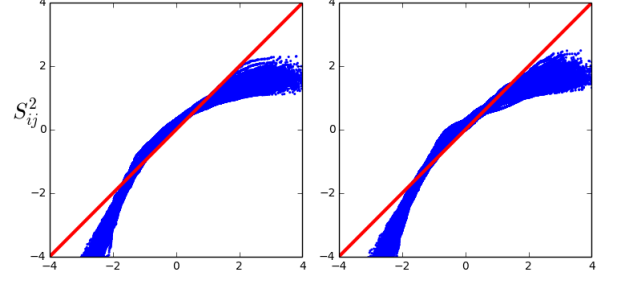


FIG. 5. Two representative QQ plots for the variables $\ln \epsilon_{1,2}$ corresponding to a diagonal (left) and off-diagonal (right) element of the matrix S . As in Fig. 1, the agreement with a log normal distribution is satisfactory up to $\pm 2\sigma$.

A LOG NORMAL MODEL FOR VELOCITY GRADIENTS

We repeat the analysis of Secs. – for the strain matrix restricted to subspaces. Let E_1 and E_2 be self adjoint projection operators on R^3 , and consider the reduced strain matrix $E_1 S E_2 = S_{1,2}$. In more detail, we consider

$$\epsilon_{1,2} = (\nu/2) \|E_1 \frac{\partial \mathbf{u}_i}{\partial x_j} E_2\|_2^2 \quad (10)$$

and the associated $\chi_{1,2} = \ln(\epsilon_{1,2})$. Thus $S_{1,2}$ is the strain associated with fluid velocities in directions spanned by E_1 and fluctuations occurring with spatial variation in directions spanned by E_2 .

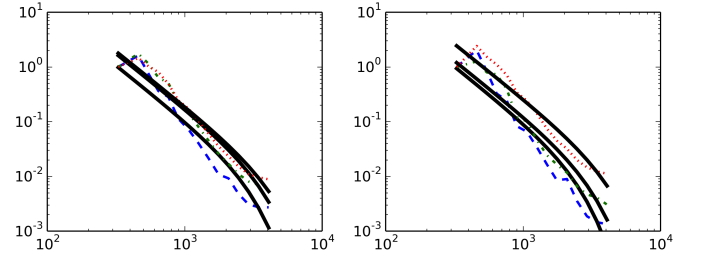


FIG. 6. The diagonal elements of $\Sigma_{1,2}^2(k)/\overline{\Sigma_{0,1,2}^2}$ plotted vs. k in $\ln \ln$ scales for two representative matrix elements of $S_{1,2}$. An $i = j$ case is presented on the left and an $i \neq j$ case presented on the right. Solid lines are the fitted curves defined in (12).

With $\hat{\mu}_{1,2}$ the rescaled resolved grid level mean for the rescaled $\hat{\chi}_{1,2}$, $\hat{\Sigma}_{1,2}^2$ is the rescaled covariance

$$\hat{\Sigma}_{1,2}^2(i_s, j_s) = n_r^{-1} \sum_{i_r} (\hat{\chi}_{1,2}(i_r, i_s) - \hat{\mu}_{1,2}(i_r)) (\hat{\chi}_{1,2}(i_r, j_s) - \hat{\mu}_{0,1,2}(i_r)) , \quad (11)$$

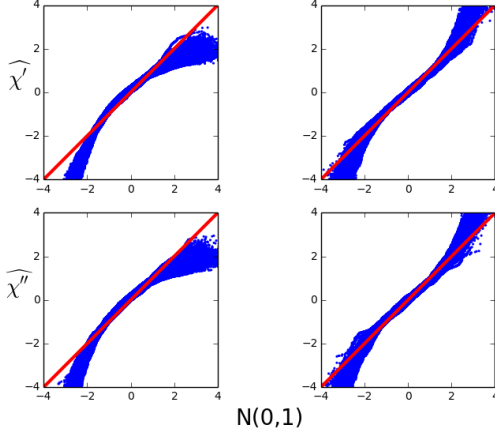


FIG. 7. The normal statistics property for representative tensor components, diagonal and off diagonal, of the χ' and χ'' tensors.

With these changes, we repeat the analysis of Figs. 1–4 with the modified dispersion relation

$$\widehat{\Sigma}_{1,2}^2(k) = \left(\dim E_1 \dim E_2 \Delta_r^3 4\pi C_{2,1,2}^2 k^2 \exp(C_{4,1,2}^2 \eta^2 k^2) \right)^{-1}, \quad (12)$$

and modified coefficients $C_{2,1,2}$ and $C_{4,1,2}$. We assume that E_1 and E_2 are both one dimensional.

We also show that the tensor dissipation operators

$$\epsilon' = (\nu/2) S^* S, \quad \epsilon'' = (\nu/2) S S^* \quad (13)$$

satisfy log normal statistics. Here the exponential and the log in the definition of log normal ($\chi' = \log(\epsilon')$ and $\chi'' = \log(\epsilon'')$) is considered in the sense of matrix operations. See Figs. 7, 8 and 9.

We note that the matrix QQ plots, and to some extent, all the QQ plots, raise the possibility of nonGaussian statistics as a correction to the normal and log normal statistics assumed here. Especially in Fig. 7, systematic corrections to the Gaussian property show smaller positive excursions and stronger negative excursions for χ than Gaussian for the diagonal matrix elements. Both the negative and positive differential excursions reflect a smaller ϵ and a possible bias toward a laminar rather than turbulent flow. In contrast, the off diagonal QQ plots suggest stronger χ excursions than Gaussian for both positive and negative excursions, a phenomena known as heavy tails in the statistical data analysis literature. These are the matrix elements which occur in vortex stretching and folding, commonly believed to be an important element of fully developed turbulence.

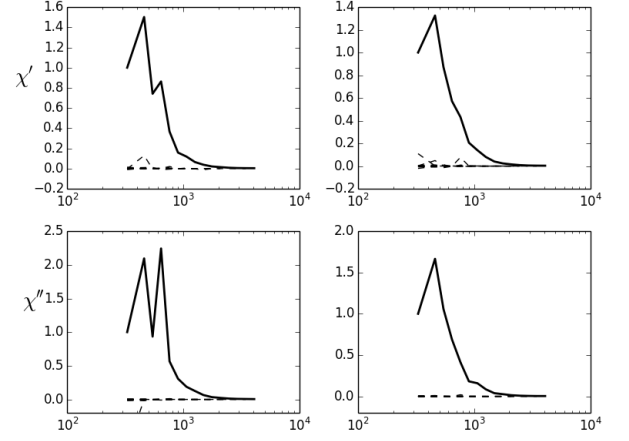


FIG. 8. The Fourier diagonal property for representative tensor components of the χ' and χ'' statistics. The two plots on the left are the diagonal components and the two on the right are off-diagonal components.

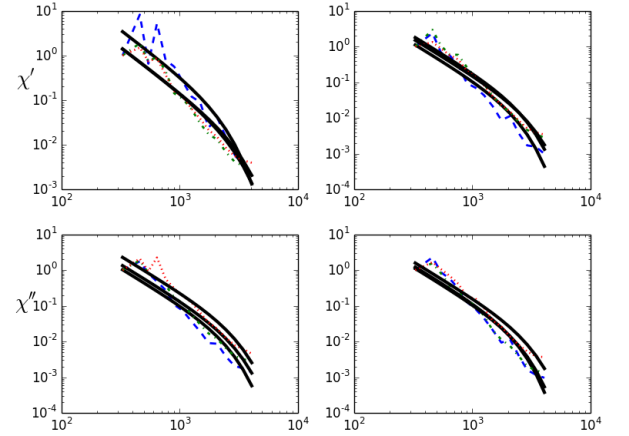


FIG. 9. The dispersion relation for representative tensor components of the χ' and χ'' statistics. The two plots on the left are the diagonal components and the two on the right are off-diagonal components.

DISCUSSION

Verification by computational studies will typically encounter only a limited range of LES unresolved scales, compared to a finely gridded simulation. But the previous analysis, when applied over many scales, has a conceptual flaw. If there is no resetting of the Σ_0^2 parameters within the statistics model of a single resolved scale, then we could apply this theory in the absence of the coarsely gridded LES to the entire computation. Doing this would remove the rescaling already seen to be important. For this reason, we restrict the model to a small range of unresolved scales. In a future publication we reformulate the model in a renormalization group manner in the case of multiple scales.

In an LES context, we analyze the unresolved scales statistically, with an emphasis on the strain rate ϵ and its logarithm $\ln \epsilon = \chi$. Resolved scale adjustments to the mean and variance for χ lead to a theory for the resulting covariance Σ^2 . We find that Σ^2 is approximately diagonal in Fourier space. An equipartition hypothesis for the variance of χ leads to a new power scaling law and a simple parameterization for Σ^2 , verified by comparison to DNS over about a decade of LES unresolved inertial scales. For reasons discussed, we restrict this theory to a single or limited range within the inertial range of scales. This pure dissipation rate model is extended to the individual velocity gradient components $\epsilon_{1,2} = (\nu/2)(\partial u_i/\partial x_j)^2$ and to the tensor dissipation rates S^*S and SS^* .

Open questions, to be addressed in future work, concern temporal statistics of turbulent intensity, statistical models for the velocity gradients and strongly nonhomogeneous flows, such as boundary layers.

[1] G. I. Barenblatt and A. J. Chorin. New perspectives in turbulence: Scaling laws, asymptotics, and intermittency. *SIAM Review*, 40:265–291, 1998.

[2] A. Chorin. *Vorticity and Turbulence*. Springer Verlag, New York–Heidelberg–Berlin, 1994.

[3] David Jou. Intermittent turbulence: a short introduction. *Scientia Marina*, 61:57–62, 1997.

[4] A. N. Kolmogorov. Local structure of turbulence in incompressible viscous fluid for very large Reynolds number. *Doklady Akad. Nauk. SSSR*, 30:299–3031, 1941.

[5] A. N. Kolmogorov. A refinement of previous hypotheses concerning the local structure of turbulence in a viscous incompressible fluid at high Reynolds number. *J. Fluid Mechanics*, 13:82–85, 1962.

[6] A. S. Monin and A. M. Yaglom. *Statistical Fluid Mechanics: Mechanics of Turbulence*. MIT Press, Cambridge, MA, 1971.

[7] A. M. Oboukhov. Some specific features of atmospheric turbulence. *J. Fluid Mech.*, 13:77–81, 1962.

[8] S.B. Pope and Y.L. Chen. The velocity-dissipation probability density function model for turbulent flows. *Phys. Fluids A*, 2, 1990.

[9] H. Pouransari, H. Kolla, J.H. Chen, and A. Mani. Spectral analysis of energy transfer in variable density, radiatively heated particle-laden flows. *Proceedings of the Summer Program, Center for Turbulence Research*, pages 27–36, 2014.

[10] K. R. Sreenivasan. Possible effects of small-scale intermittency in turbulent combustion. *Flow, Turbulence and Combustion*, 72:115–131, 2004.

[11] P. K. Yeung and S. B. Pope. Lagrangian statistics from direct numerical simulations of isotropic turbulence. *J. Fluid Mech.*, 207:531–586, 1989.